Acceleration and Extension of Radial Point Interpolation Method (RPIM) to Complex Electromagnetic Structures

Kazem Sabet[#1], Anca I. Stefan[#]
[#]EMAG Technologies, Ann Arbor, MI, USA
[1]ksabet@emagtech.com

***Abstract*—The computational performance of the radial point interpolation method (RPIM) is analyzed in highly discontinuous scenarios involving non-uniform grids as well as inhomogeneous media. A method of accelerating the RPIM simulation using domain decomposition on a high-performance computing (HPC) platform is additionally investigated. Our results indicate that RPIM may outperform FDTD where simulations of electrically large problems are concerned.**

***Keywords*—finite difference methods, interpolation, convergence of numerical methods, high performance computing, cavity resonators.**

I. Introduction

The radial point interpolation method (RPIM) has gained attention for solving electromagnetic problems in the past decade [1]-[8]. A major advantage of RPIM over the finite-difference time domain (FDTD) method lies in its ability to solve problems on sets of scattered data points, as well as complicated geometries that would otherwise lead to very refined FDTD grids, require long computation times, or initiate signal integrity issues when modeling wave propagation over large distances. RPIM uses radial basis functions (RBFs), the most commonly used scattered data interpolation technique, and is also referred to as the RBF time-domain method. The RBF expansion consists of a weighted sum of a set of shifted replicates of a single basis function. These replicates are differentiated analytically, and therefore, can be used to reduce the FDTD dispersion effects, another potential advantage over FDTD.

RPIM can overcome some of the known issues of pseudo-spectral time domain (PSTD) methods [9]. For example, the presence of the Gibbs phenomenon at the boundaries, requirement of uniform or Chebyshev-type grids, as well as computational challenges presented by large-scale problems, are all characteristic of PSTD with global or local Fourier bases.

To the authors' best knowledge, RPIM has been employed to solve relatively small and simple meshless two-dimensional and three-dimensional electromagnetic problems. Furthermore, as with any other numerical method, RPIM is not free of shortcomings. For example, late-time instability, slow convergence, and dielectric interface issues have all been reported in [5], [6], and [10]. Additionally, when solving large problems where high accuracy is required, ensuring the stability of the method becomes very critical [11].

In the work presented here, we discuss the performance of RPIM in the context of two different types of discontinuities: (a) on non-uniform Yee grids inside homogeneous media, e.g., in the proximity of a source region, and (b) inside inhomogeneous media consisting of several conjoined, lossy or lossless dielectric materials. Finally, we investigate the acceleration of RPIM using structure partitioning and domain decomposition methods. Our results highlight the potential of RPIM for efficient deployment of the solution of electrically large problems with complex geometries and material compositions on high-performance computer clusters.

II. An Overview of RPIM

Time-domain Maxwell's equations for the electric and magnetic fields are solved on a standard Yee grid by replacing the time derivatives of the field components with their RBF approximations. A brief description of the mathematical approach follows.

Consider a set of distinct points $\{x_1, \ldots, x_M\}$. These points can be part of a structured grid or they might have no geometrical relationship to one another (e.g., a scattered point cloud). An arbitrary function f is approximated by an RBF expansion as

$$f(\mathbf{x}) \approx \sum_{j=1}^{M} \lambda_j \varphi_j(\mathbf{x}). \tag{1}$$

In (1), φ_j are RBFs, λ_j are unknown coefficients, and $\mathbf{x} = [x_1 \ldots x_M]$. By enforcing the interpolation condition, that the right side of (1) match f exactly at points $\{x_1, \ldots, x_M\}$, we obtain the following system of linear equations for the unknown coefficients:

$$\begin{cases} f(x_1) = \lambda_1\varphi_1(x_1) + \cdots + \lambda_M \varphi_M(x_1) \\ \vdots \\ f(x_M) = \lambda_1\varphi_1(x_M) + \cdots + \lambda_M\varphi_M(x_M) \end{cases} \tag{2}$$

The discussion will now focus on the Gaussian RBF, as described by [12]:

$$\varphi(r, \varepsilon) = e^{-\varepsilon^2 r^2}, \tag{3}$$

where the parameter ε represents the shape parameter, and r is the radial distance. The individual RBF basis functions in (1) are now defined as

$$\varphi_j(\mathbf{x}) = e^{-\varepsilon^2 \|\mathbf{x}-\mathbf{x_j}\|^2}. \tag{4}$$

Define vectors $\mathbf{u}$ and $\mathbf{\Lambda}$, and matrix $\mathbf{A}$ as follows:

$$\begin{gathered} \mathbf{u} := [f(x_1) \ldots f(x_M)]^T \\ \mathbf{\Lambda} := [\lambda_1 \ldots \lambda_M]^T, \\ \mathbf{A}_{M\times M} : a_{ij} = e^{-\varepsilon^2 \|\mathbf{x_i}-\mathbf{x_j}\|^2}. \end{gathered} \tag{5}$$

Thus, in matrix form, (2) becomes:

$$\mathbf{u} = \mathbf{A}\mathbf{\Lambda},$$

which can be solved as

$$\mathbf{\Lambda} = \mathbf{A}^{-1}\mathbf{u}. \quad (6)$$

It follows that if matrix **A** is invertible, the coefficients λ_j in expansion (1) can be computed from the linear system solution given by (6). Furthermore, provided function f meets certain smoothness criteria, its first-order partial derivatives can be approximated as

$$\frac{\partial f(\mathbf{x})}{\partial x_k} \approx \sum_{j=1}^{M} \frac{\partial \varphi_j(\mathbf{x})}{\partial x_k} \lambda_j. \quad (7)$$

Note that, in (7), the coefficients λ_j are known, and the partial derivatives of the RBFs in this equation can be computed analytically and then evaluated at each point using definition (4) in conjunction with the derivative of (3) given by

$$\frac{\partial}{\partial r}\varphi(r,\varepsilon) = -2\varepsilon^2 r e^{-\varepsilon^2 r^2}. \quad (8)$$

In the actual RPIM simulation, the vector **u** holds the values of all the six field components at each time step. The unknown coefficients are computed using (6), and the first-order derivatives of the electric and magnetic fields are then approximated using (7) at each time step.

An alternative formulation for the Gaussian RBF includes a domain support parameter d in the following form:

$$\varphi(r,\varepsilon) = e^{-\varepsilon(r/d)^2}. \quad (9)$$

The domain support characterizes a subset of the global point set $\{x_1, \ldots, x_M\}$ that is used to approximate f, and leads to the so-called "local" RBF methods, as described in [1]-[3]. The "global" RBF poses a number of computational difficulties. First, the computation of the unknown coefficients at each iteration is the major bottleneck of the simulation, which has been reported by others, e.g. by [4]. Second, RPIM is not unconditionally stable. The shape parameter ε can be manipulated and optimized to improve accuracy [2]. However, the higher degree of approximation accuracy comes at the cost of larger conditioning numbers of the system matrix, which in turn leads to long-term instability [3]. The system matrix is well-conditioned when both the shape parameter and the minimum separation distance between points are large. Unfortunately, these two conditions cannot often be met simultaneously [13].

III. RPIM on a Non-Uniform Grid

Our test case for a non-uniform grid consists of a 2-D model of a rectangular resonant cavity structure, 0.390-m long and 0.145-m wide. Cell sizes are $\Delta x = 0.01$ m and $\Delta y = 0.005$ m. Walls are modeled as perfect electric conductors, and layers of low-loss dielectric are placed in front of the walls to ensure covergence of the solution. The structure is excited by a modulated Gaussian pulse centered at 1.546 GHz, corresponding to the third resonant mode. The excitation is located along a vertical line through the center of the structure.

RPIM simulations were run with shape parameters that were different for the x and y directions, but were maintained constant along each of the two directions. Preliminary simulations (not shown here) have confirmed that the accuracy of the method, as determined by the resonant peak value and field distributions, increases as the value of the shape parameter decreases. Accuracy also improves when the shape parameter is variable from one grid point to another. Such observations are also reported by [2]. We have also found that as the shape parameter decreases below a certain threshold, instability occurs, most likely as a result of an increase in the conditioning number of matrix **A.**

A non-uniform grid was created by step changes in the grid cell size along the x-direction as shown in Fig. 1. The non-uniform grid simulation was run with a constant shape parameter to ensure stability. As the simulation results shown in Fig. 2 indicate, RPIM performs well at this degree of grid non-uniformity. The electric field distributions compare well with the FDTD results for the same number of time steps and frequency. There were no severe "numerical" reflections or instabilities observed at the interfaces between different grid sizes.

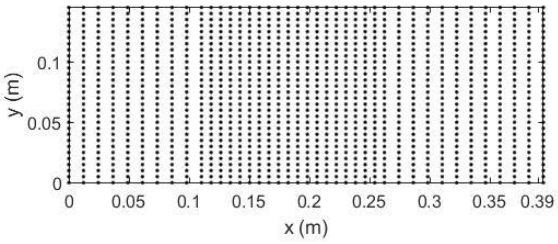

Fig. 1. A non-uniform FDTD grid. The grid is more dense in the middle of the computational domain, where the excitation source is located.

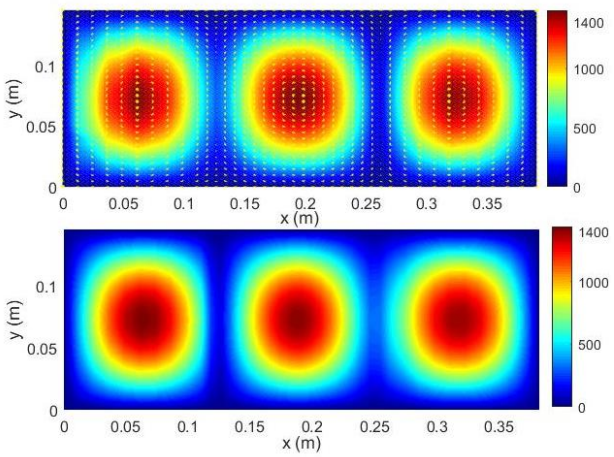

Fig. 2. Magnitude of electric field distributions in V/m. Top: Fields computed with RPIM. Bottom: Fields computed with FDTD. Simulations were run with the same number of time steps ensuring convergence. The non-uniform grid (yellow dots) is overlaid onto the RPIM results for reference.

IV. RPIM in Inhomogeneous Media

We continued our investigation of the RPIM performance with a test case consisting of the same structure described in Fig. 1, this time using a uniform mesh. Material inhomogeneity was, however, introduced in the form of a cylinder filled with three different lossy dielectric materials as shown in Fig. 3a. The relative permittivity values of the three regions were set to 2.5 (purple), 10 (white) and 12 (green), and their electric conductivity values were set to 0.02 S/m, 0.015 S/m, and 0.1

S/m, respectively. These values can be representative of a biological tissue sample.

The RPIM simulation results are presented in Figs. 3b and 3c, and again compare well with the FDTD simulation with regards to the electric field distribution. Furthermore, both methods produced the resonant peak of interest at 1.502 GHz, and were run for the same number of steps, sufficient for convergence.

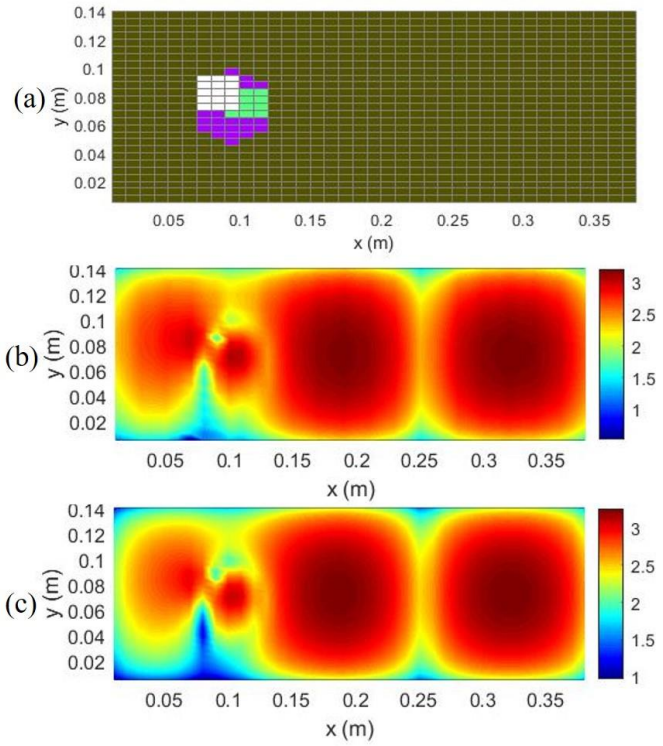

Fig. 3. Simulations with inhomogeneous media. (a) The FDTD grid with a three-region inhomogeneous cylinder; (b) Electric field distribution (dB) obtained with the RPIM simulation; (c) Electric field distribution (dB) obtained with the FDTD simulation.

V. Computational Speedup of RPIM

Our findings suggest that RPIM can be used effectively and efficiently for simulating a variety of electromagnetic structures and problems. We are particularly interested in the application of RPIM to solving electrically large problems on high-performance computing (HPC) platforms. For this type of problems, speeding up the computation is of utmost importance. In its current form, the major slowdown of our RPIM implementation is solving a linear system where the matrix has a large conditioning number. Domain partitioning was chosen as the approach to speeding up the process, whereby the computational domain is divided into a number of subdomains, and field components are matched at the boundaries of these subdomains at each time step. The subdomain computations are performed simultaneously in parallel and faster.

The computational domain described in Fig. 1 was partitioned into 2, 3, or, 4 subdomains along the x and y directions. Fig. 4 illustrates the finding that our decomposition schemes led to up to a 5x speedup. Simulations were run for 10,000 time steps; any startup overhead was assumed to be a small percentage of computation time after 10,000 steps, and therefore, the results were good estimates of the computational time. Our results indicate that, (1) domain partitioning is a viable approach to speed up the overall computation time, and (2) the speedup appears to reach a plateau when the subdomain size reaches a certain percentage of the overall computational domain size.

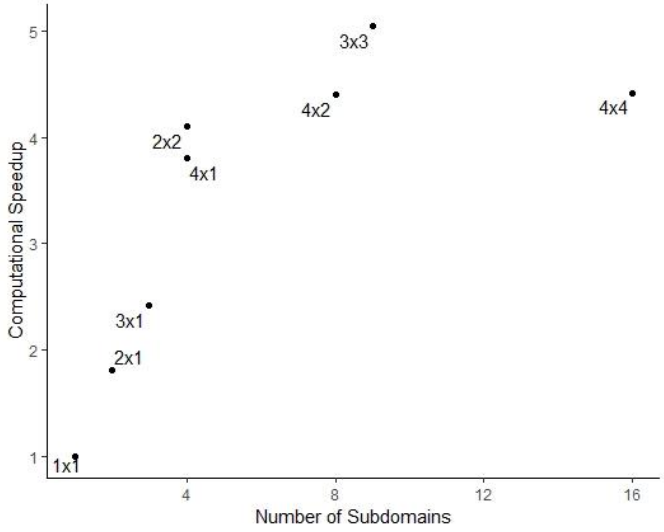

Fig. 4. Computational speedup obtained by domain partitioning. The labels on each point indicate the domain partitioning. The point labeled '1x1' represents the case with no partitioning, and is the reference.

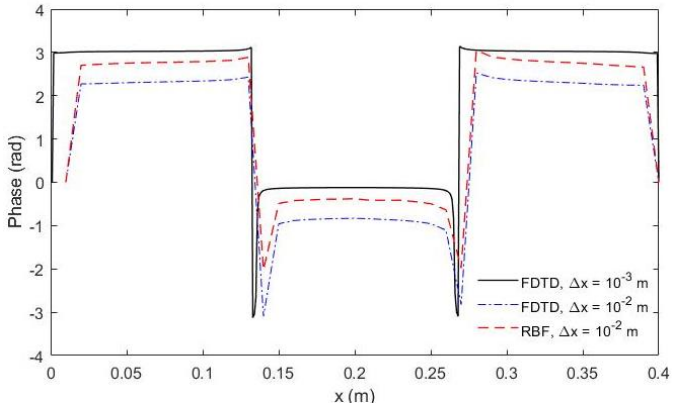

Fig. 5. The phase of the electric field along the x-direction. Comparison of RBF/RPIM results with FDTD of the same resolution and high resolution FDTD. Simulations were carried out at the resonant frequency of the third resonant mode.

Furthermore, we investigated the accuracy of RPIM combined with domain partitioning. Fig. 5 shows plots of the phase of the electric field along the x-direction computed at the resonant frequency of the third resonant mode. The figure illustrates a performance comparison of an RPIM simulation with the simplest partition (2 by 1) with an FDTD simulation for the same number of time steps (75,000). Also shown in Fig. 5 for the purpose of benchmarking are the results of a FDTD simulation of the same structure with a much higher spatial resolution (10x finer cell size), which took 500,000 time steps to converge. The "dips" seen at the discontinuity points can primarily be attributed to the presence of the lossy dielectric

layers at the right and left boundaries of the computational domain. Their presence is a slight deviation from an ideal resonant cavity, but given that the metallic walls were modeled without loss, some loss had to be introduced to ensure the convergence of the FDTD simulation. The results of Fig. 5 are encouraging, showing that not only does RPIM perform comparably to FDTD for this type of problem, but its convergence behavior is superior for a fixed number of time steps.

VI. Conclusion

We have investigated the performance of RPIM on a non-uniform structured grid, as well as on a uniform grid with inhomogeneous media. Additional simulation results involving three-dimensional resonant cavities and other types of structures will be presented at the symposium. We have found that RPIM performs comparably well or better than FDTD, and it has potential application to problems involving highly inhomogeneous and lossy media such as biological tissue. Our analysis has also shown that the RPIM method can be parallelized effectively, which along with our other findings, opens the door to solving large-scale problems with complicated geometries, such as wave propagation and penetration in urban environments at lower frequency bands. Furthermore, as the high degree of approximation accuracy of RPIM has already been recognized, we see a tremendous potential for the application of this method to problems where the minimization of phase distortion is highly desired or critical.

References

[1] Y. Yu and Z. Chen, "A 3-D radial point interpolation method for meshless time-domain modeling," IEEE Transactions on Microwave Theory and Techniques., vol. 57, pp. 2015–2020, Aug. 2009.

[2] Z. Shaterian, "Staggered and Non-Staggered Time Domain Meshless Radial Point Interpolation Method in Electromagnetics," Ph.D. dissertation, The University of Adelaide, Australia, 2015.

[3] T. Kaufmann, "The meshless radial point interpolation method for electromagnetics," Ph.D. Dissertation, ETH Zurich, Switzerland, 2011.

[4] R. Khalef, M. T. Benhabiles, F. Grine and M. L. Riabi, "An Unconditionally Stable Radial Point Interpolation Meshless Method

[5] Based on the Crank–Nicolson Scheme Solution of Wave Equation," IEEE Transactions on Microwave Theory and Techniques, vol. 66, no. 8, pp. 3705-3713, Aug. 2018.

[6] Y. Yu and Z. Chen, "Dielectric boundary conditions with the meshless radial point interpolation method," 14th International Symposium on Antenna Technology and Applied Electromagnetics & the American Electromagnetics Conference, Ottawa, ON, 2010, pp. 1-4.

[7] T. Kaufmann, C. Engström, C. Fumeaux and R. Vahldieck, "Eigenvalue Analysis and Longtime Stability of Resonant Structures for the Meshless Radial Point Interpolation Method in Time Domain," IEEE Transactions on Microwave Theory and Techniques, vol. 58, no. 12, pp. 3399-3408, Dec. 2010.

[8] S. J. Lai, B. Z. Wang and Y. Duan, "Meshless Radial Basis Function Method for Transient Electromagnetic Computations," IEEE Transactions on Magnetics, vol. 44, no. 10, pp. 2288-2295, Oct. 2008.

[9] S. Yang, Z. Chen, Y. Yu and S. Ponomarenko, "On the Numerical Dispersion of the Radial Point Interpolation Meshless Method," IEEE Microwave and Wireless Components Letters, vol. 24, no. 10, pp. 653-655, Oct. 2014.

[10] A. Taflove, Ed., A. Oskooi, and S.G. Johnson, CoEd., Advances in FDTD Computational Electrodynamics: Photonics and Nanotechnology, Artech House, 2013.

[11] S. De Marchi and R. Schaback, "Stability of kernel-based interpolation," Advances in Computational Mathematics, vol. 32, pp. 155-161, 2010.

[12] V. Scherbakov, "Localised Radial Basis Function Methods for Partial Differential Equations," Ph.D. dissertation, Uppsala University, Sweden, 2018.

[13] S. A. Sarra, "Adaptive radial basis function methods for time dependent partial differential equations," Applied Numerical Mathematics, vol. 54, pp. 79-94, 2005.

[14] R. Schaback, "Error estimates and condition numbers for radial basis function interpolation.," Advances in Computational Mathematics, vol. 3, pp. 251–264, 1995.